The Catalytic Use of Onion-Like Carbon Materials for Styrene Synthesis by Oxidative Dehydrogenation of Ethylbenzene

Nicolas Keller, Nadezhda I. Maksimova, Vladimir V. Roddatis, Michael Schur, Gerhard Mestl,* Yurii V. Butenko, Vladimir L. Kuznetsov, and Robert Schlögl*

Since the discovery of fullerenes in 1985,[1] the chemistry of sp^2-hybridized nanostructured carbon has received increasing attention both from a fundamental point of view and for potential applications. A large variety of new fullerene-related materials (giant fullerenes, nanotubes, nanospheres, nanocones, nanofolders, nanobundles, onion-like carbons (OLCs)) have been synthesized.[2] Their unique chemical and physical properties suggest novel applications, which include nanoscale engineering and electronics, optoelectronic sensors, three-dimensional composite materials, microfilters, magnetic materials, and catalysis.[3] Current research on OLCs is confined to the development of synthesis methods and to the description of physical and chemical properties.[4] These closed, spherical, carbon shells, however, could also provide interesting catalytic properties as a result of the almost perfect graphite network with a high degree of curvature.

Direct dehydrogenation of hydrocarbons is used in numerous industrial processes. Because of their endothermic character, such processes are restricted by thermodynamic limitations, thus alternatives are called for. In case of styrene synthesis, one of the ten most important industrial processes, the exothermic oxidative dehydrogenation (ODH) of ethylbenzene is an elegant and promising reaction, for which carbon catalysts have already proved their efficiency.[5, 6] The porosity of carbon catalysts used to date seems to play a negative role by hindering the styrene desorption. This effect limits the ethylbenzene conversion and leads to nonselective, consecutive reactions.[5, 7] Therefore, because of the absence of inner particle porosity OLCs are valuable candidates as catalysts.[8]

Figure 1 displays the catalytic behavior of the OLC material for the ODH of ethylbenzene to styrene with time on stream (t). For comparison, the steady-state yields are also shown, which were obtained over the industrial K–Fe catalyst and other forms of carbon. The OLC catalyst exhibited a minor initial activity developing into conversion levels of 92% after an activation period of about 2 hours on stream. The stable styrene selectivity of 68% allowed high styrene yields of 62%. The performance of OLC in ODH is not restricted as in case of traditional K-promoted iron-oxide systems, for which thermodynamic constraints limit the maximum styrene yield to 50%.[9, 10]

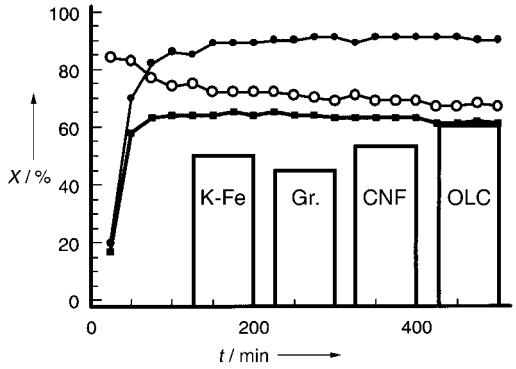

Figure 1. Performance of OLC in the ODH of ethylbenzene at 790 K with time on stream. X = ethylbenzene conversion (●), selectivity to styrene (○), and styrene yield (■). Steady-state styrene yields for graphite (Gr.), carbon nanofilaments (CNF), and the industrial K–Fe catalyst are also given. Data are given relative to the catalyst mass.

Figure 2A displays high-resolution transmission electron micrographs of fresh OLC. The left-hand image of Figure 2A shows clean, multishell particles with an interlayer distance close to 0.35 nm, typical for sp^2-hybridized carbon structures. The inset of Figure 2A shows one example of a well resolved OLC. The contrast variations of this OLC indicate not-intact graphene layers and structurally less-defined areas (indicated by arrows) of the curvature. The right-hand image displays OLC material after 40 h catalysis. The OLC seems to have disintegrated into more or less disorganized carbon.

X-ray diffraction (XRD) was further used to characterize the structure of OLC before and after catalysis. Figure 2B shows the XRD data, the diffractogram of fresh OLC is characteristic for graphite-like material with a high degree of stacking faults. For comparison in Figure 2B, the theoretical pattern of hexagonal graphite is indicated by the vertical lines with the respective indexing. The diffractogram recorded after catalysis (Figure 2B, b) demonstrates the generation of diamond-like-carbon (DLC) material, that is, sp^3-hybridized carbon atoms, during the styrene reaction. The peaks at 43.9 and 75.3° 2Θ coincide with the 111 and 220 reflections of diamond as indicated by the vertical lines. Hence, DLC is part of the ill-defined material formed during catalysis.

Figure 2C shows the Raman spectra obtained from the fresh and used OLC. The deconvolution of these spectra is displayed on the right side of Figure 2C. Spectrum (a) exhibits the Raman bands characteristic for disordered (D: 1318 cm^{-1}, and D′: 1602 cm^{-1}) and ordered (G: 1573 cm^{-1} graphene structures.[11] This Raman spectrum is in agreement with the HR-TEM analysis which revealed intact graphene layers and ill-defined structures at the curvatures of OLC (Figure 2A, left) and the XRD data (Figure 2B, pattern a). The intense Raman signature of the D (1328 cm^{-1}) and D′ (1594 cm^{-1}) bands of the catalyst after reaction, completely overwhelming the G band at 1572 cm^{-1} clearly indicate a pronounced presence of disordered carbon structures after the catalytic run. The intensity increase of the two D and D′ Raman signals was accompanied by a broadening and a slight blue-shift of

[*] Prof. Dr. R. Schlögl, Dr. N. Keller, N. I. Maksimova, Dr. V. V. Roddatis, Dr. M. Schur
Abteilung Anorganische Chemie
Fritz-Haber-Institut der Max-Planck-Gesellschaft
Faradayweg 4–6, 14195 Berlin (Germany)
Fax: (+49) 30-8413-4401
E-mail: Schloegl@fhi-berlin.mpg.de
Dr. G. Mestl
Nanoscape AG
Frankfurter Ring 193A, 80809 Munich (Germany)
Dr. Y. V. Butenko, Dr. V. L. Kuznetsov
Boreskov Institute of Catalysis
Lavrentieva 5, 630090 Novosibirsk (Russian Federation)

  1433-7851/02/4111-1885 $ 20.00+.50/0

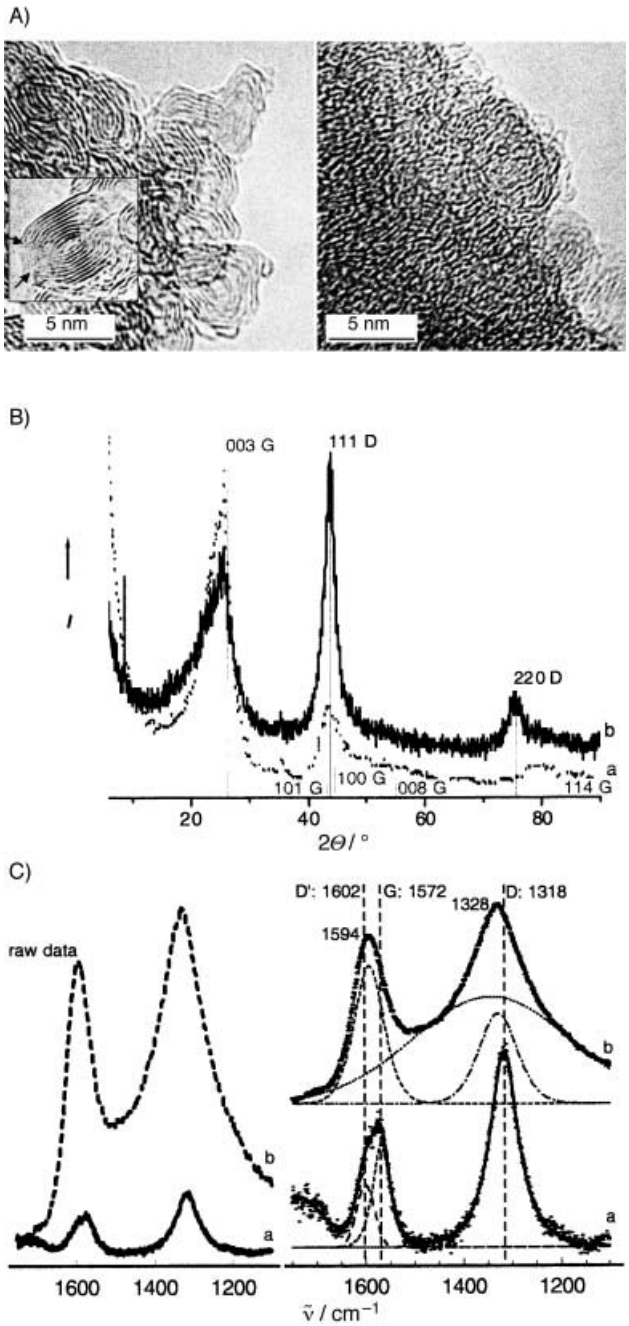

Figure 2. A) High-resolution (HR) TEM images of OLC prior (left) and subsequent to use in the ODH of ethylbenzene (right). The inset shows an enlargement of a single, intact OLC. The arrows indicate the blurred regions with less-ordered structure. B) X-ray diffractograms of the OLC material prior (a) and subsequent to catalysis (b); the calculated positions of the reflections of graphite (G) and diamond (D) are shown. C) Left: original Raman spectra (raw data) of OLC prior (a) and subsequent to use in the ODH of ethylbenzene (b); right: deconvolutions of the Raman spectra prior (a) and subsequent to catalysis (b).

the D band. The deconvolution additionally revealed a very broad background contribution to this band from C–H, C–C deformations.[12] This very broad D band does not exclude the presence of sp^3-hybridized carbon atoms after the reaction, as indicated by XRD (Figure 2B, pattern b).[12] Indeed, IR spectroscopy (spectra not shown) revealed the presence of C–H valence bands at 2920 cm^{-1} after catalysis, together with bands at 1740, 1175, and 1090 cm^{-1} which indicate the presence of basic C=O and C–O groups, respectively.

In addition to Raman spectroscopy and XRD, thermogravimetry temperature-programmed oxidation (TG-TPO) confirmed the presence of these two carbon species (Figure 3). Compared to the fresh, well-organized sp^2-hybridized OLC (Figure 3, curve a), the used catalyst displayed a

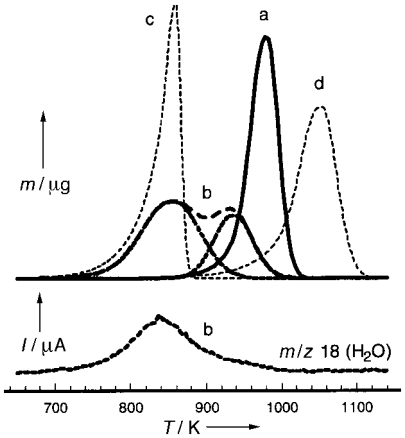

Figure 3. Differential thermal gravimetry of the temperature-programmed combustion of OLC prior (a), subsequent to use in the ODH of ethylbenzene (b), T = temperature, from amorphous carbon (c; Norit A, Aldrich), and graphite (d; SFG6, Timcal AG). Below: mass spectrometer trace of water formed during the combustion of OLC following catalysis.

composite signal (Figure 3, curve b), which indicated disordered sp^2/sp^3-hybridized carbon with a maximum combustion rate at around 850 K, in agreement with the reference sample, amorphous activated charcoal. The contribution to combustion at higher temperatures was assigned to remaining ordered sp^2-carbon structures. The water release, also at 850 K, was detected by mass spectroscopy (Figure 3, bottom) and confirmed the presence of hydrogen atoms (as indicated by IR spectroscopy) in the highly disordered carbon array.

Figure 4 shows the O1s and C1s (X-ray photoemission) XP spectra of fresh and used OLC samples. The almost oxygen-free carbon surface of the fresh OLC (Figure 4A, solid line) was transformed after reaction into an oxygen-containing surface (open circles, Figure 4A). The O1s spectrum after reaction can be deconvoluted into two signals. The first, with a binding energy (B.E.) of 530.9 eV,[13] is similar to spectra reported for other active carbon catalysts[6, 8] and is assigned to chinoidic carbonyl functions. The dehydrogenating power of the catalyst thus seems to be linked to the generation of these strongly basic sites during activation. The second with a B.E. of 533.4 eV arises from water adsorbed during transport through air. Through an increased intensity at the high-energy side of the C1s signal, the C1s spectra (Figure 4B) also indicate the presence of oxidized carbon. The inset of Figure 4B shows the difference spectrum of used OLC (full line) and fresh OLC (dotted line). Its deconvolution confirmed the presence two contributions, at 288.2, indicative for basic, chinoidic surface groups, and 286.0 eV from C–O groups. This XPS finding is in agreement with the IR spectroscopy observations mentioned above. Additionally,

  1433-7851/02/4111-1886 $ 20.00+.50/0

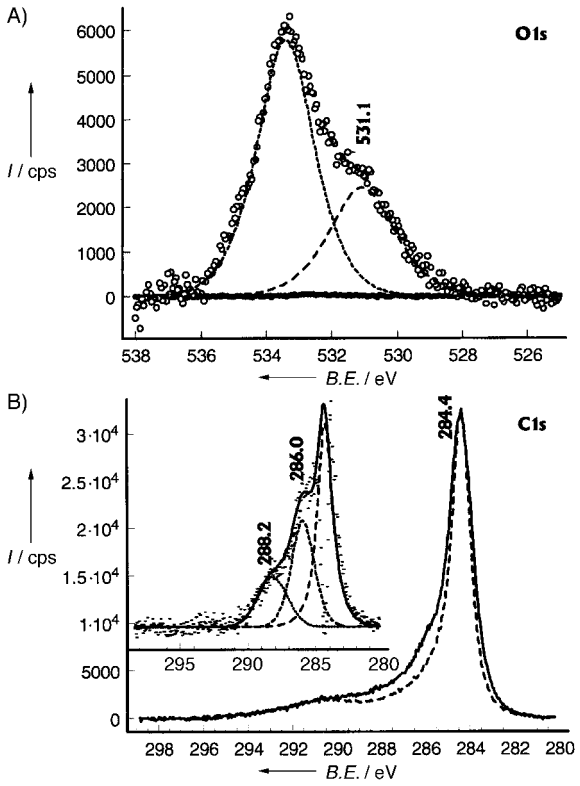

Figure 4. A) O1s XP spectra of the OLC prior (solid line) and subsequent (open circles) to catalysis. The deconvolution into two contributions with B.E. of 531.1 and 533.4 eV is shown. B) C1s XP spectra of OLC prior (dashed line) and subsequent to catalysis (full line). The inset shows the deconvolution of the difference C1s spectrum into three contributions with BE of 288.2, 286.0, and 284.4 eV.

the graphitic C1s line at 284.4 eV was considerably broadened after catalysis demonstrating the presence of structurally ill-defined carbon in line with Raman, XRD, and TG-TPO results

The structural characterization reveals that the function of the OLC as an ODH catalyst is uniquely related to its microstructure. The starting material, intact OLC with a large surface abundance of graphitic (0001) facets combined with a small abundance of edge/kink sites where the bending of the graphene layers occurs (blurred contrast in the TEM, Figure 2), is characterized by the complete absence of surface oxygen functionalities. This material does not show any catalytic activity. Catalytic activity develops with time on stream. The XP spectra indicate the generation of strongly basic, chinoidic surface functionalities on the active carbon catalyst which are responsible for the catalytic activity. These basic, dehydrogenating, surface groups are generated as resonance-stabilized C=O surface terminations of the edge/kink regions of OLC.[7] This oxidation of the edge/kink sites is also seen as being responsible for the disintegration of the OLC during catalysis. The catalytic activity develops with increasing formation of these basic functionalities and accordingly increasing OLC disintegration. Hence, it may be questioned whether OLCs are catalytically active at all. Comparative experiments with ultradispersed diamond (UDD), however, revealed that the DLC material detected by XRD after catalysis can not account for the catalytic activity of OLC (data not shown). UDD are initially also completely inactive, like OLC, but their selectivity, which develops with time, is different from that of OLC; with UDD the main product from the ODH of ethylbenzene is benzene.

That the OLC is superior in its performance to other forms of carbon (Figure 1) indicates that this type of carbon contains a higher number of active sites per unit weight at steady state. This superior performance is also related to the optimized distribution of the oxygen-activating sites (basal planes) and Brønsted basic centers (prismatic planes).[9] The presence of disordered, sp^2- and sp^3-hybridized polymeric carbon resulting from unwanted styrene polymerization is characteristic of all the catalytic systems tested so far.[9, 14] However the large volume and great number of defects in such polymeric (amorphous) species, makes them particularly susceptible to oxidation in situ (see Figure 3). As the formation of coke cannot be completely avoided a large difference in specific reactivity of the soft coke (polymeric species)[15] and the carbon catalyst is a prerequisite for stable operation. Reducing the number of basic sites, which cause polymerization, to the minimum necessary for activating the ethylbenzene substrate, makes the tendency for coke formation on carbon lower than on (potassium-promoted) metal-oxide systems.

The results reveal that a significant potential for catalytic application lies in unpromoted nanocarbon materials if their microstructure can be tailored to support the optimum distribution of electron-donating and C–H-activating functions. The chemical simplicity of carbon and the unique self-cleaning property that deactivated surfaces gasify themselves in ODH reactions, not only makes carbon species well-suited model systems but also allows realistic expectations of an industrial application in heterogeneous catalysis. The difficulties associated with the synthesis of the present OLC model system may be overcome by tailoring other more abundant forms of carbon into the desired target structure by synthetic[16] and post-synthetic thermochemical procedures.

Experimental Section

OLCs were produced by thermal annealing of UDD powder at 2140 K under a 10^{-6} torr vacuum, according to ref. [17]. The reaction was carried out in a tubular quartz reactor of 4 mm inner diameter and 200 mm length. The catalyst (0.04 g) was placed in the isothermal oven zone between quartz wool plugs. He and O_2 were fed by mass-flow controllers (Bronkhorst). Ethylbenzene in a stream of He was provided by a saturator kept at the required temperature (35 °C, corresponding to 2.16 kPa) and mixed with the O_2 flow to obtain the ethylbenzene:O_2 ratio of 1:1. The reaction was conducted at 790 K with an inlet ethylbenzene concentration of 2 vol% and a liquid hourly space velocity (LHSV) of 0.5 h^{-1}. The inlet and outlet gas analysis was carried out online by a gas chromatograph using a packed column (5% SP-1200/1.75% Bentone 34) for hydrocarbons and a capillary column (Carboxen 1010 PLOT) for permanent gases coupled to a flame ionization detector (FID) and a thermal conductivity detector (TCD), respectively.

TEM micrographs were taken on a Phillips CM200-FEG at an acceleration voltage of 200 kV. XP spectra were recorded with a modified Leybold Heraeus spectrometer (LHS12 MCD) with $Mg_{K\alpha}$ radiation (1253.6 eV) at a power of 240 W. The bandpass energy was set to 50 eV. X-ray satellites and Shirley background were subtracted. Thermal gravimetry analysis was performed on a Netzsch STA 449C balance, with a heating rate of 10 K min^{-1} and by using a 20% (v/v) O_2/He mixture, and coupled to a QMS200 mass spectrometer (Thermostar, Pfeiffer Vacuum). Raman spectra were recorded with a LabRam spectrometer (Dilor). The slit width

  1433-7851/02/4111-1887 $ 20.00+.50/0

was set at 500 μm giving a spectral resolution of 5 cm^{-1}. A He/Ne laser at 632.8 nm was used as the excitation source. IR spectra in diffuse reflectance were recorded on a Bruker IFS-66 FT-IR spectrometer. XRD was performed on a Stoe Theta-Theta diffractometer in reflection ($Cu_{K\alpha}$ radiation).

Received: July 23, 2001
Revised: March 5, 2002 [Z17567]

[1] H. W. Kroto, J. R. Heath, S. C. O'Brien, R. F. Curl, R. E. Smalley, *Nature* **1985**, *318*, 162.
[2] a) S. Iijima, *Nature* **1991**, *354*, 56; b) D. Ugarte, *Nature* **1992**, *359*, 670; c) H. O. Pierson, *Handbook of Carbon, Graphite, Diamond and Fullerenes. Properties, Processing and Applications*, Noyes Publications, Park Ridge, **1993**; d) M. Jose-Yacamau, H. Terrones, L. Rendou, J. M. Dominguez, *Carbon* **1995**, *33*, 669; e) *Carbon nanotubes: preparation and properties* (Ed.: T. W. Ebbesen), CRC, Boca Raton, **1997**; f) M. Knupfer, *Surf. Sci. Rep.* **2001**, *42*, 1, and references therein.
[3] a) M. Terrones, W. Kuang Hsu, H. W. Kroto, D. R. M. Walton, *Top. Curr. Chem.* **1999**, *199*, 189, and references therein; b) P. M. Ajayan, O. Z. Zhou *Top. Appl. Phys.* **2001**, *80*, 391.
[4] a) D. Ugarte, *Carbon* **1995**, *33*, 989; b) V. L. Kuznetsov, Yu. V. Butenko, A. L. Chuvilin, A. I. Romanenko, A. V. Okotrub, *Chem. Phys. Lett.* **2001**, *336*, 397.
[5] M. F. R. Pereira, J. J.M Orfao, J. L. Figueiredo, *Appl. Catal. A* **1999**, *184*, 153.
[6] G. Mestl, N. I. Maksimova, N. Keller, V. V. Roddatis, R. Schlögl, *Angew. Chem.* **2001**, *113*, 2122; *Angew. Chem. Int. Ed.* **2001**, *40*, 2066.
[7] a) C. Kuhrs, Y. Arita, W. Weiss, W. Ranke, R. Schlögl, *Top. Catal.* **2001**, *14*, 111; b) J. A. Maciá, D. C. Amorós, A. L. Solano, *Proceedings of the Reunión de la Sociedad Española de Catálisis*, **2001**, pp. 97–98.
[8] a) A more detailed comparison of the performances obtained with different forms of carbon will be given in a coming extended paper; b) storage in air and transfer to the XPS chamber led to a second contribution arising from adsorbed water.
[9] G. Emig, H. Hofmann, *J. Catal.* **1983**, *84*, 15.
[10] F. Cavani, F. Trifiro, *Appl. Catal. A* **1995**, *133*, 219.
[11] a) R. P. Vidano, D. B. Fishbach, L. J. Willis, T. M. Loehr, *Solid State Commun.* **1981**, *39*, 423; b) M. S. Dresselhaus, G. Dresselhaus, *Adv. Phys.* **1981**, *30*, 139; c) Y. Kawashima, G. Katagiri, *Phys. Rev. B* **1995**, *52*, 10053.
[12] D. Espinat, H. Dexpert, E. Freund, G. Martino, M. Couzi, P. Lespade, F. Cruege, *Appl. Catal.* **1985**, *16*, 343.
[13] a) H. Ago, T. Kugler, F. Cacialli, W. R. Salaneck, M. S. P. Shaffer, A. H. Windle, R. H. Friend, *J. Phys. Chem. B* **1999**, *103*, 8116; b) M. Voll, H. P. Boehm, *Carbon* **1971**, *9*, 481.
[14] G. E. Vrieland, *J. Catal.* **1988**, *111*, 14.
[15] R. Schlögl in *Handbook of Heterogeneous Catalysis*, *Vol. 1* (Eds.: G. Ertl, H. Knözinger, J. Weitkamp), Wiley-VCH, Weinheim, **1997**, pp. 138–191.
[16] C. Pham-Huu, N. Keller, V. V. Roddatis, G. Mestl, R. Schlögl, M. J. Ledoux, **2002**, *4*, 514–521.
[17] a) V. L. Kuznetsov, A. L. Chuvilin, Yu. V. Butenko, I. Y. Mal'kov, V. M. Titov, *Chem. Phys. Lett.* **1994**, *222*, 343; b) V. L. Kuznetsov, A. L. Chuvilin, E. M. Moroz, V. N. Kolomiichuk, Sh. K. Shaikhutdinov, Yu. V. Butenko, *Carbon* **1994**, *32(5)*, 873.

Tin Analogues of "Arduengo Carbenes": Synthesis of 1,3,2λ^2-Diazastannoles and Transfer of Sn Atoms between a 1,3,2λ^2-Diazastannole and a Diazadiene**

Timo Gans-Eichler, Dietrich Gudat,* and Martin Nieger

The discovery of persistent and in preparative-scale isolable carbenes launched not only a rapid development of carbene chemistry,[1] but stimulated as well investigations on carbene homologues with heavier Group 14 elements. Utilization of the concept that mesomeric interaction with the π electrons of two nitrogen atoms and a C–C double bond allows efficient electronic stabilization of the divalent carbon atom in imidazoyl ("Arduengo-type") carbenes **I**[2] lead to the isolation of analogous silylenes **II**;[3] and germylenes **III** (Scheme 1).[4] Homologues of **I** with Sn (**IV**) and Pb (**V**) are—apart from a few annellated 1,3,2λ^2-diazastannoles[5]—still unknown, although divalent compounds of these elements should become increasingly more stable descending the group from C to Pb.[6] We report here the preparation and first reaction studies of monocyclic 1,3,2λ^2-diazastannoles **IV** which reveal that the reactivity of these compounds displays some striking dissimilarities when compared to the lighter homologues **I**–**III**.

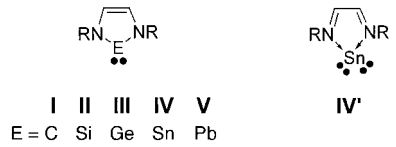

I **II** **III** **IV** **V** **IV'**
E = C Si Ge Sn Pb

Scheme 1.

λ^2-Diazagermoles **III** and annellated λ^2-diazastannoles can be prepared by metathesis of dilithiated diazadienides or *o*-phenylene diamides with $GeCl_2 \cdot$ dioxane or $SnCl_2$, respectively.[4, 5] Analogous reactions of $SnCl_2$ with the dilithiumdiamides **2a**, **b** (Scheme 2) failed,[7] but the desired monocyclic diazastannoles **7a**,**b** were found to be accessible by transamination of the α-amino aldimines **3a**,**b**[8] with $[Sn(N(SiMe_3)_2)_2]$ (**4**) at 40–45 °C in nonpolar solvents. Mechanistically, the formation of **7a**,**b** can be explained by a multistep sequence (Scheme 2) which involves the initial condensation of **3a**,**b** and **4** to give stannylenes **5**, a subsequent 1,3-H-shift to afford **6**, and finally intramolecular elimination of $HN(SiMe_3)_2$ to produce the final products **7a**,**b** which were isolated after workup as red, air sensitive, and rather thermolabile solids. Experimental support for this

[*] Prof. Dr. D. Gudat, Dipl.-Chem. T. Gans-Eichler, Dr. M. Nieger
Institut für Anorganische Chemie
Universität Bonn
Gerhard-Domagk Strasse 1, 53121 Bonn (Germany)
Fax: (+49) 228-73-5327
E-mail: dgudat@uni-bonn.de

[**] This work was supported by the Deutsche Forschungsgemeinschaft. Parts were presented as a poster at the Jahrestagung Chemie 2001 der GDCH.

  1433-7851/02/4111-1888 $ 20.00+.50/0